**PARAMETER**
JURNAL MATEMATIKA, STATISTIKA DAN TERAPANNYA

e-ISSN. 2829-6303
Vol. 05, No.1, April 2026
Pages 219-232

# EWMA Robust Max-M Control Chart for Synthetic and Real Data

**Samin Radjid[1*], Wibawati[2], Muhammad Ahsan[3]**

[1,2,3]Department of Statistics, Faculty of Science and Data Analytics, Institut Teknologi Sepuluh Nopember
ITS Raya Street, Keputih, Sukolilo, Surabaya, 60117, East Java, Indonesia.

E-mail Correspondence Author: *wibawati@its.ac.id

***Abstract***
*Quality monitoring in multivariate industrial processes requires a control chart capable of detecting changes in the process mean and variability simultaneously. This study implements the Exponentially Weighted Moving Average Robust Max-M Control Chart (ERMM-Chart) for individual multivariate observations using synthetic data and real cement clinker quality data. Robust Phase I parameter estimation is performed using the Fast Minimum Covariance Determinant method to obtain resistant estimates of the process center and covariance matrix. The synthetic data consist of four scenarios: no shift, mean shift, variability shift, and simultaneous mean-variability shift. The real data include two clinker quality characteristics, namely free lime (FCaO) and tetracalcium aluminoferrite ($C_4AF$). Results show that the ERMM-Chart produces no out-of-control signals under the no-shift scenario and detects process changes under shifted conditions. In the clinker data, the chart indicates a difference in joint process behavior between the Phase I and Phase II. Therefore, the ERMM-Chart can serve as a robust simultaneous multivariate monitoring tool for individual observations.*
***Keywords:*** *Clinker, ERMM-Chart, EWMA, Fast-MCD, robust control chart.*

: https://doi.org/10.30598/parameterv5i1pp219-232



*Email: jurnalparameter@gmail.com*
*Homepage: https://ojs3.unpatti.ac.id/index.php/parameter*

*Submitted: February 2026*
*Accepted: April 2026*

## 1. INTRODUCTION

Quality control is an essential part of industrial processes because product quality is often determined by several correlated quality characteristics. In Statistical Process Control (SPC), control charts are used to evaluate whether a process remains in an in-control condition or has shifted to an out-of-control condition that requires corrective action [1]. Therefore, a control chart is not only a visual monitoring tool but also a statistical decision-making procedure for process monitoring.

In multivariate processes, monitoring each characteristic separately using univariate control charts can be inefficient because the correlation structure among variables is not considered. When several quality characteristics change jointly, decisions based on separate charts may lead to inconsistent interpretations. Therefore, multivariate control charts are required to monitor several quality characteristics simultaneously within a single analytical framework [2]. In multivariate process monitoring, changes may occur in the process mean, the variability structure, or both. Hotelling's $T^2$ statistic is widely used to monitor the process mean, while changes in variability are commonly evaluated through the covariance matrix or other multivariate dispersion measures [3]-[6]. However, the use of separate charts for the mean and variability may complicate interpretation in practical applications. For this reason, simultaneous control charts were developed to combine information on the mean and variability into a single monitoring statistic. The idea of monitoring the process mean and variability simultaneously in one chart has also been discussed in the bivariate control chart framework [7].

The maximum-type monitoring concept was introduced through the Max-Chart framework, which combines mean and variability information in one chart [8]. This idea was later extended to the multivariate case through the Max-Mchart, which is designed to monitor the process mean and variability simultaneously [9]. For individual observations, the successive difference approach allows the variability component to be constructed without requiring subgroup data [4], [10]. This principle is used as the basis for constructing the robust Max-M statistic in this study, so that the process can still be monitored when observations are recorded individually.

In addition to simultaneous monitoring, sensitivity to small process shifts is also an important issue. The Exponentially Weighted Moving Average (EWMA) scheme, originally introduced by Roberts [11], is a memory-type control chart that uses information from current and previous observations. EWMA has been widely discussed as an effective procedure for detecting small shifts in process behavior [12], [13]. Xie [14] also showed that the sensitivity of maximum-type statistics can be improved by integrating them with the EWMA mechanism. More recently, the EWMA Max-M control chart was developed for individual multivariate observations by incorporating the EWMA mechanism into the Max-M statistic to improve sensitivity in simultaneous monitoring [15]. In practical applications, Phase I data are not always free from outliers. Outliers may distort the classical estimates of the mean vector and covariance matrix, resulting in unstable control limits. This condition may cause masking, where actual process signals are hidden, or swamping, where normal observations are incorrectly identified as out-of-control. To reduce these effects, robust estimators are needed in the Phase I parameter estimation stage. One commonly used robust estimator is the Minimum Covariance Determinant (MCD), while the Fast-MCD algorithm was developed to obtain robust estimates of location and covariance more efficiently [16], [17]. The use of Fast-MCD has also been considered in robust multivariate control chart

procedures, such as robust MEWMA, to improve resistance against outlying observations [18]. Furthermore, recent robust-chart studies have shown that robust covariance-based methods can improve the reliability of simultaneous control charts under outlier contamination [19], [20].

Based on these considerations, this study applies the Exponentially Weighted Moving Average Robust Max-M Control Chart (ERMM-Chart) to synthetic data and real cement clinker quality data. The focus of this paper is the implementation of the ERMM-Chart as an applied monitoring procedure. The synthetic data are used to examine the chart response under several shift scenarios, while the real clinker data are used to evaluate the application of the chart to actual industrial quality data involving FCaO and $C_4AF$. The contribution of this study is to demonstrate how the ERMM-Chart can be implemented as a robust simultaneous multivariate control chart for individual observations in cement clinker quality monitoring.

## 2. METHOD

### 2.1. Research Data

This study uses two types of data, namely synthetic data and real clinker quality data. The synthetic data are used to illustrate the behavior of the ERMM-Chart under several process conditions, including no shift, mean shift, variability shift, and simultaneous mean-variability shift. Each synthetic dataset consists of 100 reference-phase observations and 20 monitoring-phase observations. In Dataset 1, the Phase II remains in an in-control condition, while in Dataset 2, Dataset 3, and Dataset 4, the Phase II is generated under the corresponding shift scenarios.

The real data consist of cement clinker quality characteristics. In this study, two variables are used, namely free lime (FCaO) and tetracalcium aluminoferrite ($C_4AF$). These variables are monitored simultaneously using the ERMM-Chart because the data are recorded as individual observations. The first 30 observations are used as the Phase I for robust parameter estimation, while the next 99 observations are used as the Phase II. Thus, the total number of real observations is 129.

**Table 1. Summary of the Data Used**

| Data Type | Purpose | Variables Analyzed | Description |
|---|---|---|---|
| Synthetic Data | To illustrate signal patterns under several process conditions | Simulated multivariate observtion | Includes no shift, mean shift, variability shift, and mean-variability shift |
| Clinker Data | To apply the ERMM-Chart to real data | FCaO and $C_4AF$ | Cement clinker quality data based on individual observations |

**Table 2. Synthetic Data Scenarios**

| Dataset | Phase I | Phase II | $a$ | $b$ | Description |
|---|---|---|---|---|---|
| 1 | In-control | In-control | 0 | 1.0 | No shift |
| 2 | In-control | Out-of-control | 2.2 | 1.0 | Mean shift |
| 3 | In-control | Out-of-control | 0 | 2.8 | Variability shift |
| 4 | In-control | Out-of-control | 2.2 | 2.8 | Mean and variability shift |

In **Table 2**, $\boldsymbol{a}$ denotes the magnitude of the mean shift, while $b$ denotes the multiplier of the covariance matrix.

### 2.2. Implementation of the ERMM-Chart Statistic

The ERMM-Chart is implemented through three computational stages: robust Phase I parameter estimation, calculation of the robust Max-M statistic, and EWMA smoothing. Let $\boldsymbol{x}_i$ denote the $i$-th observation vector with dimension $p$, where $i = 1,2,\dots,n$. In the Phase I, robust estimates of the process center and covariance matrix are obtained using the Fast-MCD algorithm.

Let $\tilde{\boldsymbol{\mu}}$ denote the robust estimate of the process center and $\tilde{\boldsymbol{\Sigma}}$ denote the robust estimate of the covariance matrix. These estimates are used as the monitoring reference in order to reduce the influence of outlying observations in Phase I. In this paper, the use of Fast-MCD is treated as a robust estimation step before the ERMM statistic is calculated

$$\tilde{U}_i = \Phi^{-1}\left[H_{\chi_p^2}\{(\boldsymbol{x}_i - \tilde{\boldsymbol{\mu}})^T\tilde{\boldsymbol{\Sigma}}^{-1}(\boldsymbol{x}_i - \tilde{\boldsymbol{\mu}})\}\right], \qquad i = 2,3,\dots,n. \tag{1}$$

where $\Phi^{-1}(\cdot)$ denotes the inverse cumulative distribution function of the standard normal distribution and $H_{\chi_p^2}(\cdot)$ denotes the cumulative distribution function of the chi-square distribution with $p$ degrees of freedom.

For individual observations, the variability component is calculated using successive differences. The robust variability component is defined as

$$\tilde{V}_i = \Phi^{-1}\left[H_{\chi_p^2}\left\{\frac{1}{2}(\boldsymbol{x}_i - \boldsymbol{x}_{i-1})^T\tilde{\boldsymbol{\Sigma}}^{-1}(\boldsymbol{x}_i - \boldsymbol{x}_{i-1})\right\}\right], \quad i = 2,3,\dots,n. \tag{2}$$

The factor $\frac{1}{2}$ is used because, under the in-control condition, the successive difference $(\mathbf{x}_i - \mathbf{x}_{i-1})$ has covariance $2\boldsymbol{\Sigma}$. Therefore, the quadratic form is scaled so that it follows the chi-square reference distribution.

The robust simultaneous Max-M statistic is then obtained by combining the mean and variability components as

$$\tilde{M}_i = \max\left(|\tilde{U}_i|, |\tilde{V}_i|\right). \tag{3}$$

Thus, $\tilde{M}_i$ summarizes the information from the robust mean component and the robust variability component into a single monitoring statistic. A large value of $\tilde{M}_i$ indicates that the $i$-th observation may deviate from the reference condition either in the mean component, the variability component, or both.

The EWMA mechanism is then applied to $\tilde{M}_i$. The ERMM statistic is calculated as

$$Z_i = \lambda\tilde{M}_i + (1-\lambda)Z_{i-1}, 0 < \lambda \leq 1, \tag{4}$$

where $Z_i$ is the EWMA-smoothed robust Max-M statistic and $\lambda$ is the EWMA weighting parameter. A smaller value of $\lambda$ gives more weight to past observations and produces a smoother chart, while a larger value of $\lambda$ gives more weight to the most recent observation and produces a more responsive chart. The initial value $Z_1 = \mu_{\tilde{M}_i}$.

Because $\tilde{M}_i$ is non-negative, the ERMM-Chart uses an upper control limit. In this study, the control limit is determined according to the parameter combination used in each application. The general form of the steady-state upper control limit is written as

$$UCL = \mu_{\tilde{M}_i} + L\sigma_{\tilde{M}_i}\sqrt{\frac{\lambda}{2-\lambda}}, \tag{5}$$

where $\mu_{\widetilde{M}_i}$ and $\sigma_{\widetilde{M}_i}$ are the center and scale parameters of the Max-M statistic, and $L$ is the control limit constant. In implementation, the process is declared out-of-control if

$$Z_i > UCL.$$

This paper focuses on the implementation of the above statistic for synthetic and real data. Therefore, the detailed derivation of the distribution of the Max-M statistic is not repeated, and the control limits are used as operational limits for evaluating the monitoring results.

### 2.3. Implementation Procedure

The implementation parameters used for the synthetic data are presented in **Table 3.** In this table, $p$ denotes the data dimension, $\rho$ denotes the correlation coefficient used in the in-control covariance matrix, $\lambda$ denotes the EWMA weighting parameter, $\alpha_{MCD}$ denotes the proportion of observations used in the Fast-MCD subset, $L$ denotes the control limit constant, and UCL denotes the upper control limit. Phase I sample size refers to the number of observations used for robust parameter estimation, while Phase II sample size refers to the number of observations used for process monitoring.

The upper control limit (UCL) of the ERMM-Chart was determined using Monte Carlo simulation under the in-control condition. The in-control process was assumed to follow a multivariate normal distribution with mean vector $\boldsymbol{\mu}_0 = 0$ and covariance matrix $\boldsymbol{\Sigma}_0$, where the diagonal elements are equal to 1 and the off-diagonal elements are equal to the correlation coefficient $\rho = 0.5$. For each value of the EWMA weighting parameter $\lambda$, a large number of in-control datasets were generated using the same Phase I and Phase II structure as the synthetic data application. The ERMM statistic $Z_i$ was then calculated for each simulated dataset using Fast-MCD estimates obtained from Phase I.

The target in-control average run length was set to $ARL_0 = 370$, which corresponds to a false alarm probability of approximately $\alpha = 1/370 = 0.0027$. Therefore, the UCL was selected as the empirical $(1-\alpha)$-quantile of the simulated in-control ERMM statistics. In this study, the quantile used was approximately 0.9973. This procedure was repeated separately for $\lambda = 0.1$, $\lambda = 0.5$, and $\lambda = 0.7$, because different EWMA weighting parameters produce different distributions of $Z_i$. The resulting values of $L$and UCL are reported in **Table 3**.

**Table 3. ERMM-Chart Implementation Parameters for Synthetic Data**

| $p$ | $\rho$ | $\lambda$ | $\alpha_{MCD}$ | $L$ | UCL | Phase I | Phase II |
|---|---|---|---|---|---|---|---|
| 5 | 0.5 | 0.1 | 0.75 | 2.617 | 1.490295 | 100 | 20 |
| 5 | 0.5 | 0.5 | 0.75 | 3.506 | 2.348581 | 100 | 20 |
| 5 | 0.5 | 0.7 | 0.75 | 3.528 | 2.688960 | 100 | 20 |

Based on **Table 3**, the UCL changes according to the value of the EWMA weighting parameter. When $\lambda = 0.1$, the UCL is 1.490295. When $\lambda$ increases to 0.5, the UCL becomes 2.348581. Furthermore, when $\lambda = 0.7$, the UCL increases to 2.688960. This pattern indicates that each value of $\lambda$ must be paired with its corresponding UCL.

The implementation procedure for the synthetic data is as follows:

a. Determine the initial parameters, including $p$, $\rho$, $\lambda$, $\alpha_{MCD}$, $L$, and UCL.
b. Define the in-control mean vector and covariance matrix.
c. Generate 100 Phase I and 20 Phase II observations from the in-control multivariate normal distribution with scenario, namely no shift, mean shift, variability shift, or simultaneous mean-variability shift.
d. Combine the Phase I and Phase II observations into one dataset.

e. Estimate $\tilde{\boldsymbol{\mu}}$ and $\tilde{\boldsymbol{\Sigma}}$ from the Phase I using Fast-MCD.
f. Calculate $\tilde{U}_i$, $\tilde{V}_i$, and $\tilde{M}_i$ for each observation.
g. Apply the EWMA mechanism to $\tilde{M}_i$ to obtain $Z_i$.
h. Compare each $Z_i$ value with the corresponding UCL.
i. Identify in-control and out-of-control observations.
j. Record the false alarms, first signal observation, Run Length (RL), and number of out-of-control signals.
k. Evaluate the detection performance of the ERMM-Chart for each dataset and each value of $\lambda$.

The implementation procedure for the real clinker data is as follows:
a. Prepare the cement clinker quality data containing FCaO and $C_4AF$.
b. Check the data structure, observation order, and missing values.
c. Divide the data into 30 Phase I observations and 99 Phase II observations.
d. Determine the parameter combination, including $\lambda$, $L$, and UCL.
e. Estimate $\tilde{\boldsymbol{\mu}}$ and $\tilde{\boldsymbol{\Sigma}}$ from the Phase I using Fast-MCD.
f. Calculate $\tilde{U}_i$, $\tilde{V}_i$, and $\tilde{M}_i$ for each observation.
g. Apply the EWMA mechanism to $\tilde{M}_i$ to obtain $Z_i$.
h. Compare each $Z_i$ value with the corresponding UCL.
i. Identify in-control and out-of-control observations.
j. Record the false alarms, first signal observation, Run Length (RL), and number of out-of-control signals.
k. Present the ERMM control chart for each value of $\lambda$.
l. Evaluate the monitoring results based on the signal pattern, RL, and number of out-of-control signals as indications of process changes in the joint behavior of FCaO and $C_4AF$.

## 3. RESULTS AND DISCUSSION

### 3.1. Application of the ERMM-Chart to Synthetic Data

The first application is conducted on synthetic data to evaluate the response of the ERMM-Chart under several process conditions. The synthetic data are designed to represent four monitoring situations, namely no shift, mean shift, variability shift, and simultaneous mean-variability shift. Each dataset consists of 120 observations, divided into 100 reference-phase observations and 20 monitoring-phase observations. The Phase I is assumed to represent the in-control process condition and is used to estimate the robust process parameters and control limits. Meanwhile, the Phase II is used to evaluate the ability of the ERMM-Chart to detect process changes after a shift is introduced. Through this design, the performance of the chart can be observed from the emergence of out-of-control signals, the number of detected signals, and the Run Length required to detect the first signal in the Phase II. Run Length (RL) in the Phase II indicates the number of observations required from the beginning of the Phase II until the first out-of-control signal is detected. A smaller RL indicates faster detection of a process shift, while a larger RL indicates that the chart requires more observations before the first signal appears. Run length and average run length are commonly used to evaluate the detection behavior of multivariate control charts [21]. In Dataset 1, the RL is not reported because the Phase II is not shifted and no out-of-control signal is detected.

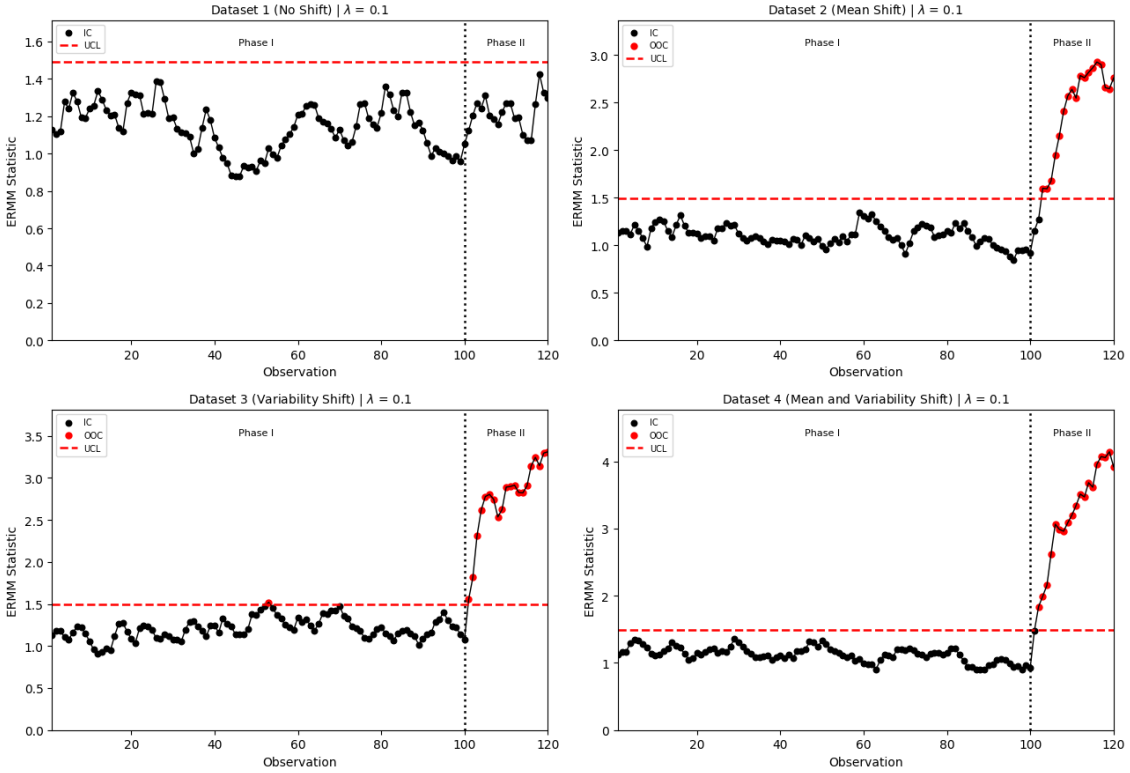


**Figure 1.** ERMM-Chart for synthetic data with $\lambda = 0.1$

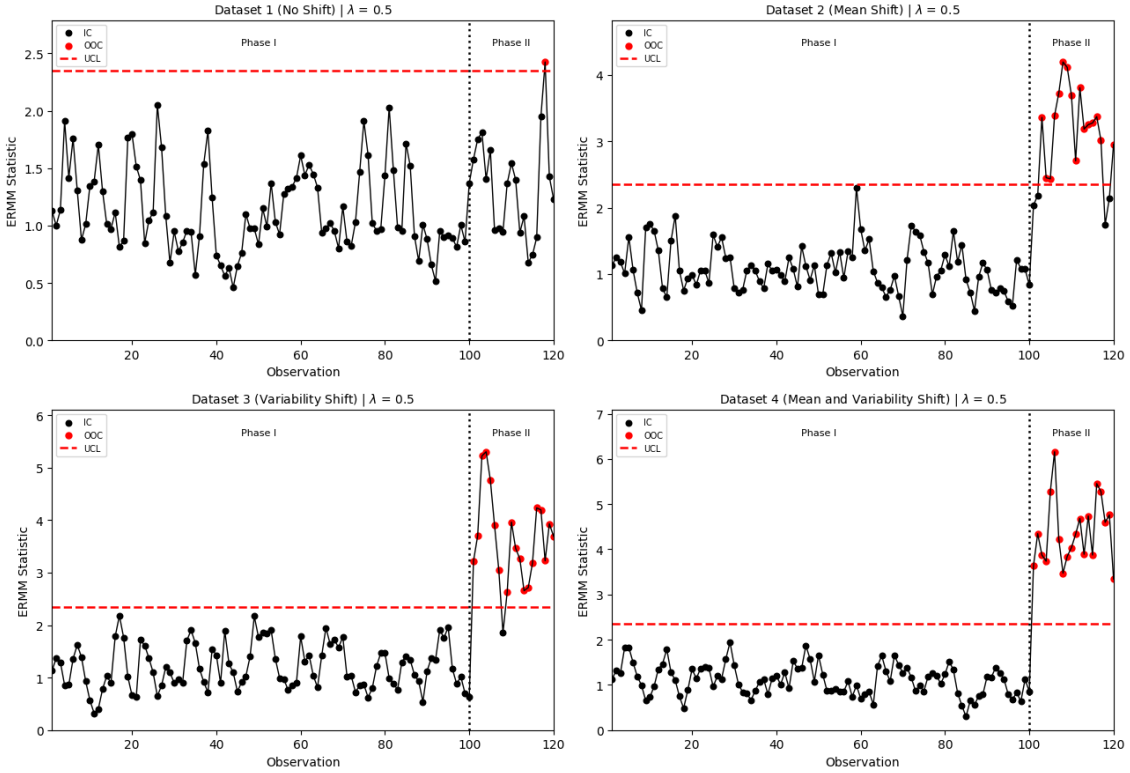


**Figure 2.** ERMM-Chart for synthetic data with $\lambda = 0.5$

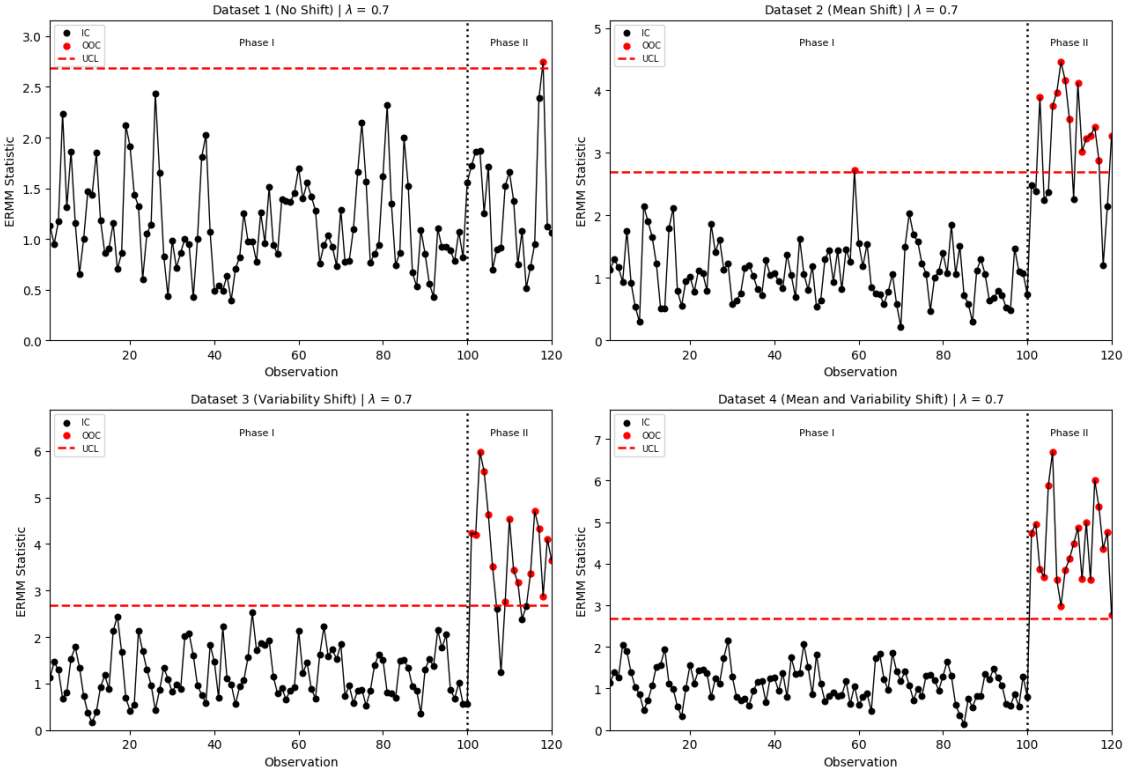


**Figure 3.** ERMM-Chart for synthetic data with $\lambda = 0.7$

**Table 4.** Summary of ERMM-Chart Detection Results for Synthetic Data

| Dataset | $\lambda$ | False Alarm (Phase I) | First Signal (Phase II) | RL (Phase II) | OOC (Phase II) | OOC Total |
|---|---|---|---|---|---|---|
| Dataset 1 (No Shift) | 0.1 | 0 | 0 | 0 | 0 | 0 |
| Dataset 2 (Mean Shift) | 0.1 | 0 | 103 | 3 | 18 | 18 |
| Dataset 3 (Var Shift) | 0.1 | 1 | 101 | 1 | 20 | 21 |
| Dataset 4 (Both Shift) | 0.1 | 0 | 102 | 2 | 19 | 19 |
| Dataset 1 (No Shift) | 0.5 | 0 | 118 | 18 | 1 | 1 |
| Dataset 2 (Mean Shift) | 0.5 | 0 | 103 | 3 | 16 | 16 |
| Dataset 3 (Var Shift) | 0.5 | 0 | 101 | 1 | 19 | 19 |
| Dataset 4 (Both Shift) | 0.5 | 0 | 101 | 1 | 20 | 20 |
| Dataset 1 (No Shift) | 0.7 | 0 | 118 | 18 | 1 | 1 |
| Dataset 2 (Mean Shift) | 0.7 | 1 | 103 | 3 | 13 | 14 |
| Dataset 3 (Var Shift) | 0.7 | 0 | 101 | 1 | 16 | 16 |
| Dataset 4 (Both Shift) | 0.7 | 0 | 101 | 1 | 20 | 20 |

**Table 4** summarizes the detection results of the ERMM-Chart for the synthetic datasets. In Dataset 1, which represents the no-shift condition, no signal was detected when $\lambda = 0.1$. However, one Phase II signal appeared for $\lambda = 0.5$ and $\lambda = 0.7$. Since Dataset 1 was generated from the in-control multivariate normal distribution without any imposed shift, these signals are interpreted as isolated false signals due to random sampling variation, not as actual process changes. In Dataset 2, the mean shift was detected for all values of $\lambda$, with the first Phase II signal appearing at observation 103, corresponding to RL = 3. The number of Phase II out-of-control signals decreased from 18 to 13 as $\lambda$ increased from 0.1 to 0.7, indicating that larger $\lambda$ values produced fewer sustained signals in this dataset. In Dataset 3, the variability shift was detected immediately at the first Phase II observation for all values of $\lambda$, with RL = 1. This shows that the ERMM-Chart is sensitive to changes in the covariance structure. Meanwhile, Dataset 4, which contains simultaneous mean and variability shifts, also produced a strong response, with RL = 2 for $\lambda = 0.1$ and RL = 1 for $\lambda = 0.5$ and $\lambda = 0.7$. Overall, the ERMM-Chart was able to detect mean shifts, variability shifts, and simultaneous shifts in Phase II. The fastest detection occurred in the variability-shift and simultaneous-shift scenarios, while the mean-shift scenario required a slightly longer run length. The occurrence of isolated false signals also indicates that the selection of $\lambda$ should consider both detection sensitivity and false-signal stability.

### 3.2. Application of the ERMM-Chart to Cement Clinker Data

The second application is conducted on real cement clinker quality data using two variables, namely FCaO and $C_4AF$. These two variables are monitored simultaneously using the ERMM-Chart. The first 30 observations are used as the Phase I for robust parameter estimation, while the following 99 observations are used as the Phase II. Since ERMM is a simultaneous statistic, an out-of-control signal indicates a dominant deviation in the mean component, the variability component, or both from the combination of the two variables.

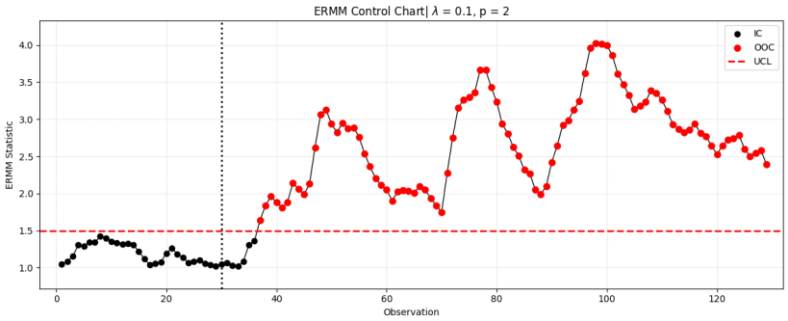


**Figure 4. ERMM-Chart for clinker data with $\lambda = 0.1$**

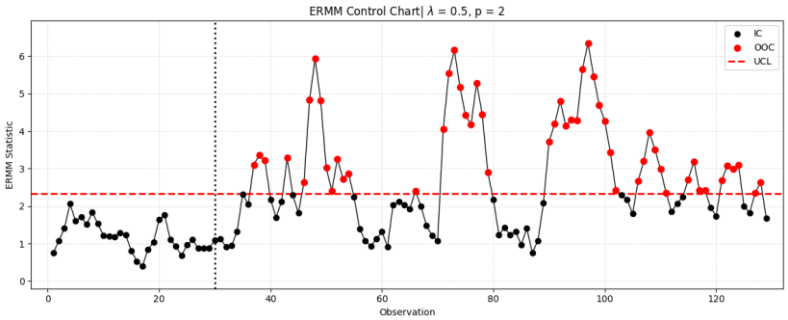


**Figure 5. ERMM-Chart for clinker data with $\lambda = 0.5$**

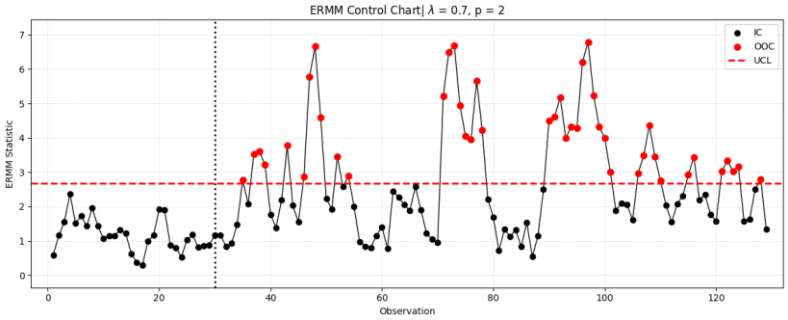


**Figure 6. ERMM-Chart for clinker data with $\lambda = 0.7$**

Based on the three values of $\lambda$, the application to clinker data shows that the ERMM-Chart can indicate process changes in the Phase II. Since two quality variables are used simultaneously, the interpretation of the signals should be directed toward the joint behavior of FCaO and $C_4AF$. The signals do not directly identify the responsible variable, so further analysis is needed to determine whether the deviation is dominated by FCaO, $C_4AF$, the mean component, the variability component, or a combination of these components.

**Table 5. Summary of ERMM-Chart Detection Results for Clinker Data**

| $\lambda$ | $L$ | UCL | False Alarm in Phase I | First Signal Observation in Phase II | RL | OOC Signals in Phase II | Total OOC Signals |
|---|---|---|---|---|---|---|---|
| 0.1 | 2.668 | 1.49734 | 0 | 37 | 7 | 93 | 93 |
| 0.5 | 3.478 | 2.33883 | 0 | 37 | 7 | 52 | 52 |
| 0.7 | 3.521 | 2.68586 | 0 | 35 | 5 | 43 | 43 |

For the real clinker data, no false alarms are found in the Phase I for all values of $\lambda$. In the Phase II, the numbers of OOC signals are 93 for $\lambda = 0.1$, 52 for $\lambda = 0.5$, and 43 for $\lambda = 0.7$. The RL values are 7, 7, and 5, respectively, indicating that the first signal appears faster at $\lambda = 0.7$. These results show that the Phase II has a different process pattern from the Phase I based on the combination of FCaO and $C_4AF$.

The large number of OOC signals in the Phase II suggests that the monitoring-phase observations have a different pattern from the Phase I. The highest number of signals is obtained at $\lambda = 0.1$, indicating that a smaller weighting parameter produces a more sensitive chart. On the other hand, $\lambda = 0.7$ produces fewer total OOC signals but gives the fastest first detection based on the RL value. Thus, the interpretation of the clinker data should consider both the number of OOC signals and the RL value. The implementation results show several advantages of the ERMM-Chart for quality monitoring based on individual observations. First, the chart can monitor the process mean and variability simultaneously in a single statistic. Second, the use of Fast-MCD makes the reference-phase parameter estimation more resistant to outliers. Third, the EWMA mechanism provides flexibility through the parameter $\lambda$, so that the chart response can be adjusted according to the type of change that is prioritized. However, the ERMM-Chart serves as an early detection tool, not as a diagnostic tool for identifying the direct cause of the signal. After an out-of-control point is detected, further examination is still required, for example by tracing $\tilde{U}_i$ and $\tilde{V}_i$, evaluating the contribution of each variable, and linking the signal to production process conditions. Therefore, the ERMM-Chart should be used as part of a quality monitoring system supported by follow-up investigation procedures.

## 4. CONCLUSION

This study applied the Exponentially Weighted Moving Average Robust Max-M Control Chart (ERMM-Chart) to synthetic data and real cement clinker quality data. The ERMM-Chart was constructed from the robust Max-M statistic and the EWMA mechanism, allowing simultaneous monitoring of changes in the process mean and variability for individual multivariate observations. The Phase I parameters were estimated using Fast-MCD to obtain robust estimates of the location vector and covariance matrix. For the synthetic data, the ERMM-Chart produced different responses according to the process scenarios. In Dataset 1, which represents the no-shift condition, no out-of-control signal was detected for $\lambda = 0.1$, while one Phase II signal appeared for $\lambda = 0.5$ and $\lambda = 0.7$. Since Dataset 1 was generated from the in-control multivariate normal distribution, these signals were interpreted as isolated false signals due to random sampling variation rather than actual process shifts. In Dataset 2, the mean shift was detected for all values of $\lambda$, with the first Phase II signal appearing at observation 103, corresponding to RL = 3. In Dataset 3, the variability shift was detected immediately at the first Phase II observation for all values of $\lambda$, corresponding to RL = 1. In Dataset 4, the simultaneous mean and variability shift produced the strongest response, with RL = 2 for $\lambda = 0.1$ and RL = 1 for $\lambda = 0.5$ and $\lambda = 0.7$. These results indicate that the ERMM-Chart is more sensitive to variability shifts and simultaneous shifts than to mean shifts alone. However, several isolated false signals were observed, so the choice of $\lambda$ should consider the balance between detection sensitivity and chart stability. For the real cement clinker data, the ERMM-Chart was applied using two quality variables, namely FCaO and $C_4AF$. The results showed no false alarms in Phase I for all values of $\lambda$. In Phase II, the numbers of out-of-control signals were 93 for $\lambda = 0.1$, 52 for $\lambda = 0.5$, and 43 for $\lambda = 0.7$. The corresponding RL values were 7, 7, and 5, indicating that the first signal appeared fastest when $\lambda = 0.7$. These findings indicate a different process pattern between Phase I and Phase II in the joint monitoring of FCaO and $C_4AF$. Overall, the ERMM-Chart can be used as a robust simultaneous multivariate control chart for industrial quality monitoring based on individual observations. Nevertheless, the out-of-control signals produced by the chart are multivariate in nature and do not directly identify the responsible variable. Further research may focus on variable contribution analysis, more detailed ARL-based performance evaluation, and comparison with other multivariate control charts.


### Acknowledgments

The authors would like to thank the Department of Statistics, Faculty of Science and Data Analytics, Institut Teknologi Sepuluh Nopember, for the academic support provided during this study.

### Funding Information

Authors state there is no funding involved.


### Author Contributions Statement

Samin Radjid: Conceptualization, methodology, software, formal analysis, visualization, and writing-original draft. Wibawati: Supervision, validation, and writing-review & editing. Muhammad Ahsan: Supervision, methodology, validation, and writing-review & editing. All authors discussed the results and contributed to the final manuscript.

### Conflict of Interest Statement

Authors state no conflict of interest.

## Informed Consent

Not applicable.

## Ethical Approval

Not applicable.

## Data Availability

The data that support the findings of this study are available from the corresponding author upon reasonable request.

## REFERENCES


[1] D. C. Montgomery, *Introduction to Statistical Quality Control*, 8th ed. Hoboken, NJ, USA: John Wiley & Sons, 2020.

[2] C. A. Lowry, W. H. Woodall, C. W. Champ, and S. E. Rigdon, "A multivariate exponentially weighted moving average control chart," *Technometrics*, vol. 34, no. 1, pp. 46–53, 1992, doi: 10.1080/00401706.1992.10485232.

[3] H. Hotelling, "Multivariate quality control, illustrated by the air testing of sample bombsights," in *Techniques of Statistical Analysis*, C. Eisenhart, M. W. Hastay, and W. A. Wallis, Eds. New York, NY, USA: McGraw-Hill, 1947, pp. 113–184.

[4] M. B. C. Khoo and S. H. Quah, "Multivariate control chart for process dispersion based on individual observations," *Quality Engineering*, vol. 15, no. 4, pp. 639–642, 2003, doi: 10.1081/QEN-120018394.

[5] M. A. Djauhari, "Improved monitoring of multivariate process variability," *Journal of Quality Technology*, vol. 37, no. 1, pp. 32–39, 2005, doi: 10.1080/00224065.2005.11980298.

[6] M. A. Djauhari, M. Mashuri, and D. E. Herwindiati, "Multivariate process variability monitoring," *Communications in Statistics - Theory and Methods*, vol. 37, no. 11, pp. 1742–1754, 2008, doi: 10.1080/03610920701826286.

[7] M. B. C. Khoo, "A new bivariate control chart to monitor the multivariate process mean and variance simultaneously," *Quality Engineering*, vol. 17, no. 1, pp. 109–118, 2004, doi: 10.1081/QEN-200028718.

[8] G. Chen and S. W. Cheng, "MAX chart: Combining X-bar chart and S chart," *Statistica Sinica*, vol. 8, pp. 263–271, 1998.

[9] K. Thaga and L. Gabaitiri, "Multivariate Max-Chart," *Economic Quality Control*, vol. 21, no. 1, pp. 113–125, 2006, doi: 10.1515/EQC.2006.113.

[10] R. Kruba, M. Mashuri, and D. D. Prastyo, "The effectiveness of Max-Half-Mchart over Max-Mchart in simultaneously monitoring process mean and variability of individual observations," *Quality and Reliability Engineering International*, vol. 37, no. 6, pp. 2334–2347, 2021, doi: 10.1002/qre.2860.

[11] S. W. Roberts, "Control chart tests based on geometric moving averages," *Technometrics*, vol. 1, no. 3, pp. 239–250, 1959, doi: 10.1080/00401706.1959.10489860.

[12] J. S. Hunter, "The exponentially weighted moving average," *Journal of Quality Technology*, vol. 18, no. 4, pp. 203–210, 1986, doi: 10.1080/00224065.1986.11979014.

[13] J. M. Lucas and M. S. Saccucci, "Exponentially weighted moving average control schemes: Properties and enhancements," *Technometrics*, vol. 32, no. 1, pp. 1–12, 1990, doi: 10.1080/00401706.1990.10484583.

[14] H. Xie, "Contributions to qualimetry," Ph.D. dissertation, University of Manitoba, Winnipeg, MB, Canada, 1999.

[15] M. Ahsan, K. A. F. Rifki, M. Mashuri, Wibawati, and M. H. Lee, "Enhanced monitoring of process anomalies: exponentially weighted moving average max multivariate (EWMA Max-M) control chart," *The International Journal of Advanced Manufacturing Technology*, vol. 139, no. 9–10, pp. 4441–4455, 2025, doi: 10.1007/s00170-025-16113-6.

[16] P. J. Rousseeuw, "Least median of squares regression," *Journal of the American Statistical Association*, vol. 79, no. 388, pp. 871–880, 1984, doi: 10.1080/01621459.1984.10477105.

[17] P. J. Rousseeuw and K. Van Driessen, "A fast algorithm for the minimum covariance determinant estimator," *Technometrics*, vol. 41, no. 3, pp. 212–223, 1999, doi: 10.1080/00401706.1999.10485670.
[18] Z. Li, R. Miao, C. Q. Wei, Z. F. Li, and Z. B. Jiang, "A robust MEWMA control chart based on FAST-MCD algorithm," *Advanced Materials Research*, vol. 562–564, pp. 1907–1911, 2012, doi: 10.4028/www.scientific.net/AMR.562-564.1907.
[19] F. Fahri, M. Ahsan, and Wibawati, "Simultaneous robust Max-Half-Mchart control charts based on minimum regularized covariance determinant (MRCD)," *AIP Conference Proceedings*, vol. 3301, no. 1, Art. no. 050008, 2025, doi: 10.1063/5.0262295.
[20] A. P. R. Sembada, M. Ahsan, and Wibawati, "Advanced process monitoring in ordinary portland cement (OPC) data using robust Max-Half-Mchart control charts with Fast-MCD and Det-MCD estimators," *AIP Conference Proceedings*, vol. 3301, no. 1, Art. no. 050006, 2025, doi: 10.1063/5.0262293.
[21] A. Javaheri and A. A. Houshmand, "Average run length comparison of multivariate control charts," *Journal of Statistical Computation and Simulation*, vol. 69, no. 2, pp. 125–140, 2001, doi: 10.1080/00949650108812086.